

**EAGLE Internal Note
MUON-NO-003**

The Honeycomb Strip Chamber as Muon Detector for EAGLE

**H. van der Graaf, NIKHEF-H, Amsterdam
A. König, Univ. of Nijmegen & NIKHEF**

Version 1, April 1992

Index

Introduction and Principle	3
The segmentation of the muon detector	5
The chambers	5
chamber geometry	5
chamber construction	5
chamber performance	6
time resolution from wire data	6
spatial resolution from wire data	6
spatial resolution from strip data	6
multiplicity and track separation;	
EM shower contamination, count rate	6
count rate	7
Chamber electronics	7
front end wires	7
TDCs	7
front end strips	7
ADCs	7
the transputer	8
The Trigger	8
level 0	8
level 1 'wire'	8
level 1 'strip'	8
Bunch Identifier	8
level 2	9
Counting room electronics	9
Mechanical Support and Alignment	9
Chamber Support	9
Alignment	9
Detector Calibration	10
T-zero calibration	10
Strip Preamp gain calibration	10
Additional systems	11
HV systems	11
gas systems	11
power supplies (low voltage)	11
cabling and tubing	11
monitor systems	11
cooling	11
data acquisition	11
off-line analyses	11
Quantities	12
Material Cost Estimates	13
Chamber Material	13
Readout Electronics	13
Other materials	14
Labour costs	14
Production facilities	15
R & D	15
Alternatives	16
References	16

Introduction and Principle

Introduction.

The muon detector identifies muons and measures muon track positions. It may provide for a trigger for muons with tracks pointing to the interaction region as well as a trigger for muons with a momentum higher than an adjustable threshold.

The muon detector consists of a magnetized iron toroid with two detection layers both at the inside and at the outside. There is a (central) barrel part and of two (forward) cap sections, together covering a rapidity of 3. The barrel detector consists basically of four coaxial cylinders built from position sensitive chambers. The assembly of the two inner cylinders, called Muon Station 1 (MS1), is positioned in the gap between the hadron calorimeter and the iron toroid. The two outer cylinders (MS2) are positioned outside the toroidal magnet. Each of the four cylinders consists of chambers which are an assembly of a number of 'monolayers'. Such a chamber is called a superlayer. The distance between the two superlayers of MS1 is as much as the gap allows. In MS2 the spacing is limited to the available space of the experimental zone.

With this detector geometry the track angle difference can be measured of the muon arriving and leaving the iron toroid. The change of the track angle is inverse proportional to the muon momentum and proportional to the integral of B^*dl .

For low momentum muons, multiple scattering limits the momentum resolution of the muon detector. For high muon momenta the errors in track position measurements, like chamber alignment and chamber spatial resolution form limiting factors in the accuracy.

In addition to the toroid, a solenoidal magnet of 2 T is placed around the interaction point. An iron yoke shapes the return field. Muon tracks in the (R, ϕ) projection have an 'S' shape. An accurate measurement of the ϕ coordinate improves the muon momentum resolution, even if the 'small solenoid' option is chosen. The strip readout of the HSCs can provide for this accurate measurement.

The momentum resolution is favoured by additional information on the muon track position measured by the inner tracker, as well as knowledge about the position of the interaction point.

In the forward and backward regions the muon momentum is measured using additional toroids. The readout system should be capable to handle the higher count rate.

Eagle is a very large experiment; since the muon detector is located at the outer regions, the surface to be covered by position sensitive muon detectors is in the range of 5000 m². Given this quantity and given the demands for spatial resolution, time resolution, count rate and track separation, the detector should be cost effective in the first place. Experience with a small prototype and from 25 'monolayers' in TRACAL, RD5, learned us that Honeycomb Strip Chambers (HSCs) are accurate, reliable and can be produced rapidly at low cost.

For the HSCs the material costs are low since only bulk materials are used (mylar foil, mold-injected plastic pieces), whereas the labour costs are limited because of the automated production and the simplicity of the concept. The HSC is therefore an excellent candidate for low-cost, large area muon detectors.

If both the strips and the wires are read out, time and amplitude (and therefore dE/dX) information is available. Given the option of using additional information, the muon detector has a good potential for discoveries in 'new physics'.

In this paper we present many details like geometry, segmentation and principles of electronics. Doing this, we would like to stress that these are only possibilities; no optimization of parameters like gas mixture, occupancy, chamber mode of operation and cell radius has been carried out. Detailed simulation of the muon detector in EAGLE will be needed before a realistic design can be made. Notably, the contamination of muons with electrons created in pair production/EM showers is essential in these simulations; the detector response should be central in this study. In addition, the RD5 facility will play a crucial role in the verification of these simulations.

Principle.

The HSC is described in detail in [1]. Hexagonal conducting rings around an anode wire pick up the positive induced charge from ions (see fig.1). These ions are the remains of an avalanche on the wire and was initiated by the free electrons created in the gas by a passing muon. The charge distribution over the strips is a function of the centroid of the ion cloud which is, in its turn, closely related to the ϕ coordinate of the track.

The hexagonal rings are formed by metal strips on folded foil: two of these foils forming a mirror image are fixed together. Such a 'cell layer', covered by a (third) flat foil forms a 'monolayer' which has some rigidity. A stack of, for instance, four monolayers glued together forms a stiff, self supporting chamber. The anode wires are positioned in the centre of each hexagonal cell. The wire tension is taken by the cell walls.

The distance between the track and the avalanche wire can be measured by recording the drift time of the free electrons. After combining the data of all chamber layers the left-right ambiguity of each hit cell can be solved and the track position can be established in terms of θ and Z .

The fact that the spatial resolution of the ϕ coordinate worsens with ϕ (see below) makes it impossible to have the HSC orientation in which the toroidal bending of the muon tracks measured by the strips. Since both the track coordinates are to be known, the strips are running in parallel to the beam, while the wires are in the direction of the toroidal magnetic field.

Given the known drift times and, after some calculations, the drift distances, the timing of the muon can be calculated and the machine bunch in which the muon was created can be identified. With this information an effective filter against cosmic rays can be obtained and a level 1 trigger can be produced. This task can, however, be done in a more straightforward way by a fast RPC trigger detector.

The strong points of HSCs as muon detector are:

- low costs;
- easy to make;
- little amount of material: light, easy to handle chambers;
- accurate two-dimensional readout; very high precision (50 - 100 μm) in ϕ coordinate;
- auto calibration possible for the Z (= drift) coordinate;
- left-right ambiguity can be solved;
- no relevant influence of magnetic field on the ϕ coordinate;
- reliable operation: no strong electric fields except around the anode wire;
- no dependency of the measured track ϕ coordinate (into the wire direction) on gas mixing ratio, temperature, pressure;
- non-flammable simple gas can be used (Ar/CO₂);
- multiplexing ADC and TDC on the chamber; optical fibre links replace all signal cables;
- can produce, if necessary, a level 1 trigger;
- can produce a level 2 trigger using accurate track position data;

The weak point of HSCs are:

- resolution in ϕ worsens with ϕ ;
- the track separation is limited to the wire pitch (12 mm) in one direction and to about three strip pitches (15 mm) in the other direction.
- the large number of readout channels

These problems are solved by:

- a 32-fold chamber segmentation in ϕ : this limits the maximum angle of incidence to 0.1 rad;
- by leaving some space between the inner superlayers in the muon stations and by a sufficiently small wire pitch. The contamination of muon tracks by electrons from EM showers can then be sufficiently low.
- given the low occupancy, multiplexers can be applied. The electronics per channel is therefore limited to one amplifier and a discriminator and only a small fraction of a TDC or ADC. ASICs are now available which limit the cost to 5 Sfr/ch and is expected to lower to 2 Sfr/ch.

The chamber performance would be improved for both coordinates if Xe gas could be applied and/or if the chamber could be operated with higher gas pressures. These options seem feasible; they could be an item of an upgrade.

The segmentation of the muon detector

The chamber length (which equals one or two times the strip length) is limited by the allowed noise level of the strip signals which is directly related to the strip capacity. A strip length of 4 m seems possible; the chamber length may be twice the strip length by having the strips read out at both strip ends while breaking the strips in the centre.

In order to have a spatial resolution better than 100 μm for the track coordinate measured by the strips, the angle of incidence φ must be smaller than 0.1 rad. This requires a 32-fold segmentation of the full circle in φ . At present, EAGLE has a 8-fold segmentation. If HSCs are applied and if a good spatial resolution in φ is required, a 16-fold segmentation of the toroid is needed. If the φ coordinate can be measured with enough accuracy by the RPCs, the HSC turns into an array of drift tubes. The segmentation of EAGLE is then of no importance and the chamber length (perpendicular to the wires) is determined merely by practical considerations. In this paper we assume the need for a good spatial resolution in φ .

Per segment the muon stations have a box shape. As a consequence, the chambers are broken in two parts (see fig.2). This reduces the effective lever arm to about 80 percent of the gap size, unless the segmentation in φ of EAGLE is 32-fold.

The edges of the superlayers with corresponding φ are displaced such that they don't line up to the interaction point. The barrel section is therefore hermetically efficient for muon detection. Dead zones at the edges and chamber sides may only cause a local loss of momentum resolution.

Fig.3 shows the side view of EAGLE: here the projected chamber segmentation in Z is indicated. Again, the dead zones of the chambers are covered by other chamber layers. In the forward regions the high density of muon tracks at high rapidity dictates the maximum lengths of wires and strips. Additional superlayers may compensate the high occupancy due to the high count rate in regions near the beam pipe.

The EAGLE muon detector can be built from 'Super Module' units. In fig.3 the 9 basic units are shown. In the Z-mirror image of EAGLE there are 9 mirror images of these units, so there are 18 different SuMos. The 16 segments of EAGLE could therefore be built from 288 SuMos.

The Chambers

Chamber Geometry.

Fig. 4 and fig.5 show the geometry of the basic multilayer chamber. The chamber consists of four or eight active monolayers. Two layers without wires are added; they stiffen the chamber and have a shielding function. The width (wire length) of the chambers varies between 2.0 m for the 'broken' chambers in MS1 to 3.6 m for the outer chambers in MS2. The length (= strip length) of the chambers is 3 - 4 m.

Chamber construction. The sequence of the chamber construction is as follows:

- purchase mylar foil with a layer of sputtered copper from industry;
- print the etch resistive ink in the strip pattern on the copper (printing is done by industry);
- etch the foil where there is no ink; remove the ink after this (done by industry);
- fold the foil in a folding machine; it turns into a 'ribbon' foil;
- put the ribbon foil on a template; a vacuum between the foil and the template provides for a firm fixation of the foil. Verify the straightness of the strips by means of a wire as reference. The ribbon foil is now in its final shape*;

* The straightness of the strips is determined by 1) the accuracy of the image cylinder which prints the etch-resistant ink (typical values: strip width 13 μm RMS, strip pitch 18 μm RMS); 2) by displacements of the foil in the printing machine (less than 50 μm over 20 m); 3) by the parallelism of the folds (better than 1 μrad) and 4) by the precision of the template (20 μm).

- glue plastic blocks (mold-injected, industrial) at the sides where the cells end on top of the foil edge. Fix the blocks by means of clamps temporarily on the template. All blocks at one side of the template form a continuous plastic strip over the entire chamber length.
- fix a square frame on the template carrying pre-mounted wires. Shift the wires in brass 'wire clips'. Compress the wire clips; the wire is fixed.
- put a second ribbon foil in a second template. Turn this template upside down. Put glue on the upper side of the plastic side strip. Lower the second template on the first template using mechanical guides.
- fix the upper and lower ribbon foils together by means of ultrasonic welding (the upper template has access holes for this purpose).
- remove the vacuum from the upper template and remove it. Glue a flat foil on top of the upper ribbon foil.
- mount the rectangular tubes at the sides of the foil where the strips end.
- remove the vacuum of the lower template; remove the finished monolayer and store it.
- put a monolayer on a flat surface. A second monolayer is mounted on top of it using adhesive tape or glue. Add all monolayers in an identical way.
- mount 'hedge-hog' printed circuit boards against the plastic chamber facings;
- seal the chamber gas tight along the outer edges, the hedge-hog boards, the panels and the tubes at the strip ends.
- mount: front end electronics, HCDs, HTDs, transputer, connections for HV, preamp power, gas. The chamber is ready for tests.

Mylar foil expands in a humid atmosphere; if the chamber is operational the foils will be dried by the chamber gas. During the assembly of the flat foils the final overall dimensions are fixed. This foil should therefore be dry during this procedure.

Chamber performance.

Time resolution from wire data. The timing obtained from the wire signals follows the typical time spectra of proportional tubes. The maximum drift time has a value of 60 - 350 ns, depending on the gas mixture. The time resolution per cell, after track reconstruction, is 4 - 10 ns, depending on the gas mixture.

Spatial resolution from wire data. Typical values for this geometry are 120 - 300 μm per cell. If special gases are applied (Xe, CF₄, DME), or if higher gas pressures are used, resolutions better than 100 μm have been reported [2,3,4]. This is an average: the resolution for tracks close to the wires is worse due to the statistical fluctuations in the cluster positions and cluster sizes of the primary electrons along the muon track.

The distance between the chamber centre planes within the muon stations is 0.6 m. The angular resolution σ_θ of a station is therefore 0.18 mrad, taken in account non-efficiencies due to the dead zone between adjacent cells and EM shower pollutions. The spatial resolution of the Z coordinate measured by one station (consisting of two superlayers) is about 60 μm .

Applying Xe gas will improve the spatial resolution by 20 - 40 percent, depending on the track position in a cell. A high pressure operated chamber will also perform better.

Spatial resolution from strip data. The spatial resolution in the ϕ coordinate of muon tracks depends on ϕ [1]. Since the full circle of EAGLE is covered by 32 chamber sections, the angle of incidence ϕ is limited to $-0.1 < \phi < 0.1$. Integration learns that the average spatial resolution of a monolayer is 80 μm , whereas the worst resolution is 100 μm . We assume therefore a spatial resolution of 100 μm . Only the inner superlayer is equipped with a strip readout system. The spatial resolution in the ϕ coordinate measured by a station is about 55 μm . If Xe gas is applied, the spatial resolution will improve by 30 percent; the worsening of the resolution with ϕ is reduced with the same factor. If the chambers would be operated using a gas pressure of 4 bars (Ar/CO₂), the spatial resolution would be improved by a factor 2.

Multiplicity and track separation: EM shower electron contamination. The read out electronics can be made such that two or more tracks within a group of 64 strips or wires can be treated separately. The number of hits per group of wires or group of strips is determined by the number of TDC and ADC units, respectively, associated with the groups.

Tracks with a distance projection in ϕ larger than 1 mm can be recognised from the widening of the charge distribution over the strips. This effect is used to veto EM shower contaminated measurements [7].

If the spacing is larger than 15 mm, both tracks can be analysed. The corresponding track separation in Z must be larger than the wire spacing (12.7 mm) in order to be recognised as a double track in Z. A GEANT simulation has shown that the inner superlayers have each a probability of 3 % to have all its monolayers measuring wrongly. The wrong measurement is recognisable from a deviation of the precisely known charge distribution over the strips [7]. Given the four points of measurement and the fact that the outer superlayers in the stations are not contaminated, the redundancy of the muon track measurements allows a reconstruction with the required precision. Furthermore, the zig-zag drift direction in the monolayers within one superlayer will result in correct measurements by about half of the number of monolayers. This will reduce the figure of contaminated measurements, to be verified in the RD5 experimental set up.

If two closely spaced muons pass the four superlayers one has in general the problem of ambiguity; there are four possibilities. The dead zone between two adjacent cells within a monolayer offers a good possibility to solve this ambiguity. The track pattern of non-hit layers is identical for the strips and for the wires. A muon passes 24 monolayers in total, each with a probability of 15 percent to cross a dead zone. This results in a probability of 75 percent that a particular layer has either a hit for both tracks or no hit for both tracks. The chance that the two track 'footprint' hit patterns of 24 bits are identical in about 0.1 percent of the two track events. This may be a powerful tool for off-line analyses.

The ADC data from three strips close to the track allows the calculation of the avalanche pulse height which is a measure for dE/dX .

Count rate. The maximum count rate depends on the group size of strips and wires which are read out by one Honeycomb Charge Digitiser (HCD) or one Honeycomb Time Digitiser (HTD), respectively. Typical figures are groups of 64 strips and 64 wires; this corresponds with 1.2 m^2 and 1.4 m^2 , respectively. A typical maximum track frequency for the HCDs and HTDs is 100 kHz.

Chamber electronics

Front end wires. Each wire is equipped with a preamp and a discriminator: these may well be integrated in a multichannel ASIC [6]. The discriminator outputs of a group of 64 wires are added in an analog summer (see fig.6). The output of this summer is fed into the inputs of four comparators which are set at different levels. The first wire that fires its discriminator will activate the first comparator. The comparator output clocks the latch: the 'chamber time' is read and stored. If a second wire fires within the active period of the first wire, the second output appears at the summer output on top of the first one. The summer output is therefore twice as high and the second latch is activated. In this way a track multiplicity of four is possible. A set of latches is applied in parallel in order to store the 'hit wire' pattern.

TDCs. The Machine Clock (66.67 MHz) is interpolated with a factor 8 into bins of 1.87 ns. By means of a 12-bit counter a 'chamber time' is generated. The chamber time repeats after $15.36 \mu\text{s}$ which is well over the processing time of a chamber hit. At the moment that a discriminator is activated, the chamber time is read in a latch.

Front end strips. Each strip of the 'inner' superlayers is equipped with a charge sensitive preamplifier. It has a low noise combined with a very large input capacity in order to receive the largest part of its strip charge. The strip capacity is in the order of 1 nF. Given the large amount of strips, 'Application Specific Integrated Circuits (ASICs) must be applied. An example may be a type developed in Brookhaven for the LAr calorimeter [5].

The amplifier is followed by the 'Combo Discriminator'. This device actually contains two discriminators: one has its two inputs connected to the outputs of two adjacent strip preamps. It reacts if $Q_{\text{left}} < Q_{\text{middle}}$. The second discriminator reacts if $Q_{\text{middle}} > Q_{\text{threshold}}$. If both discriminators react, the output of the combo disc is activated. A priority decoder at the outputs of the discriminators detects the most-right activated combo disc. This one is associated with the strip carrying the largest signal Q_{middle} .

The activated output of the priority encoder opens two groups of three analog switches (see fig.7) associated with Q_{left} , Q_{middle} and Q_{right} . The signals appear on the 'analog backbone'. These three signals are converted using three FADCs.

Preamps and combo discs as ASIC are mounted at the end of the strips. ADCs just behind the front end PCB. A parallel bus transports the data from the FADCs and the data which identifies the strip carrying Q_{middle} to the transputer.

ADCs. The three analog signals Q_{left} , Q_{middle} and Q_{right} are fed into three FADCs. One of these ADCs converts the signal Q_{middle} in an conventional way. The other two FADC have Q_{middle} as common reference signal and Q_{left} and Q_{right} as inputs, respectively. Their outputs are therefore the ratios $Q_{\text{left}}/Q_{\text{middle}}$ and $Q_{\text{right}}/Q_{\text{middle}}$. The wire pulse height can be calculated from the ADC data, providing for additional selection possibilities like energy loss and pulse height discrimination.

By adding sets of analog switches, the number of analog backbones can be extended, thus providing for multi-hit capacity.

The transputer. Each group of two chambers forming a segment of a station, is equipped with a transputer. It has the following tasks: a) it controls the data flow between the chambers and the counting room; b) it prepares the data for trigger 2; c) it controls calibration and test procedures and d) it controls monitor data streams such as the sensing of temperature and magnetic field.

The chamber transputer has optical links to other transputers in the segment, to the counting room and to trigger 2 which may consist of transputers as well.

The Trigger

level 0

Each station section (with total number of 12 layers) has its own level 0 trigger which is activated if half of the chamber layers or more had a hit within a period of maximum drift time. The 'OR' outputs of the wire front end serve as inputs for this trigger, the (digital) signals are simply added by means of a fast opamp. The output of this opamp is put into a comparator which has an adjustable threshold. This comparator will react as soon as enough layers had a hit, no matter where the hits actually took place in each layer.

level 1 'wire' (optional: this trigger can be obtained from RPCs)

Each of the 16 segments has its own level 1 trigger; it has inputs for the adjacent segments as well. This enables to process tracks leaving one segment and entering a neighbour.

This trigger has the 'hit wire' data as input. By means of lookup tables the hit wire data is converted into figures for angle θ . A corresponding bit is set in an array which is binned in θ horizontally and in all the chamber layers of all four stations vertically. Tracks, originating from the interaction point result in this array as a straight line; its angle is a measure for the muon momentum. By means of vertical majority logic a valid track is detected.

The trigger is supposed to decide after 1 μs .

level 1 'strips' (optional).

Parallel to the level 1 trigger which uses hit wire information, a trigger could be used which uses the 'maximum' strips. This data is available in the same way as the 'hit wire' data.

Accurate ADC information can be used after 1.5 μs . By means of some look-up tables the sagitta could be known after about 2 μs . This would allow a sharp low-momentum cut-off in trigger level 1.

Bunch Identifier (optional: this information can be obtained from RPCs in a more simple way).

After the drift time interval, the wire gives a signal. At this moment the clock is read and latched. This figure is the sum of the drift time and a time T_0 which is equal for all the hit wires, associated with the same track (disregarding time of flight and signal propagation delays). It is easy to see that the sum of the recorded times of two adjacent chamber layers equals roughly the maximum drift time plus two times T_0 . Corrections are needed for non-perpendicular incident tracks. The difference between the two drift times is a function of the track positions within the cells. The combination of the sum and difference can give the value for T_0 .

This system could consist of stacks of lookup tables. First the hit wire data is converted in an angle θ . This data is combined with the clock data of two adjacent layers; the lookup table has the track timing as an output. This process takes place in parallel for each combination of two hit adjacent planes.

The accuracy of this timing should be better than 5 ns (RMS; bunch crossing each 15 ns = 3σ). Given the present timing resolution of 4 - 10 ns per chamber layer the Bunch Identifier seems feasible.

As an alternative the drift times can be processed simultaneously in a number of processors, each with a 15 different T-zero. The number of processors needed equals the maximum drift time divided by 15 ns, corresponding with the number of possible bunches. The processors fit a straight line touching circles around the wires. The processor which arrives at the lowest chi-square 'wins'. A group from the University of Utrecht is studying the application of neural networks for this problem.

The propagation delay of signals over the wires should be taken into account (max 20 ns).

The bunch identifier is supposed to decide after 1 μ s.

level 2

After a positive level 1 trigger, the ADC data from the strips is read out and guided to the 2nd level trigger. This trigger consists of transputers and is located near the stations 4. It is segmented, like the other triggers, and capable of handling segment-crossing tracks. Using the ADC data, an accurate track position is calculated for a few chamber layers. After this the muon momentum is calculated and compared with the momentum threshold. Communication between the level 2 transputers and the blockhouse electronics will result in the detection of one or more (coincident) muons. The level 2 trigger could be generated after 1 ms.

Counting room electronics

In the counting room housing is needed for:

- 350 receivers for optical fibres (ie transputers),
- the muon online host computer
- HV power supplies and distribution panels,
- Monitor systems for the High & Low Voltage power supplies.

Mechanical Support and Alignment

Chamber Support

Each SuMo is a self-supporting unit consisting of a multi-layer RPC, an 8-layer 'inner' HSC and a 4-layer 'outer' HSC. Depending on the applied alignment system, the three chambers may be fixed together in a very rigid way, thus providing for an internally aligned unit. As an alternative, the chamber fixation may only provide for the relative spacing in Y, leaving flexibility in X and Z. The latter two can be defined by the applied alignment systems.

The HSCs can be made thermically stable by covering them with a thin carbon fibre laminate or a thin glass plate. This may lead to a less demanding alignment system.

A SuMo itself can be fixed using three feet. The feet can be equipped with wheels, allowing to run a row of SuMOS in their position.

Alignment.

We assume that the accuracy of the wire positions and width and pitch of the strips on the foil is such that it is of no influence on the track position measurements (values obtained are 15 μ m for the wire positions, 13 μ m for the strip width and 18 μ m for the strip pitch). The chambers may be stiffened by carbon or glass fibre planes, reducing the effects of thermal and moisture expansion.

During the production of the chamber layers the straightness of the strips is verified and, if necessary, corrected for. The layers are kept in a rigid frame during production and storage.

During the assembly of chamber layers, no special care will be taken for the relative alignment of the chamber layers. As has been shown [7], the relative alignment of the chamber planes can be obtained, due to the good spatial resolution in both directions, from about 1000 perpendicular tracks (for instance in a cosmic ray station). Three variables (Z1, Z2 and X) per chamber layer are derived from the track data, describing the alignment of a layer. The data, obtained in one night of cosmic rays will provide for the 12 and 24 figures associated with a four-layer and eight-layer chamber, respectively. These are to be stored in a data base.

Each superlayer will have reference planes which will define the chamber position in the cosmic ray station. Precision rods against these reference planes will define the chamber or monolayer position in the experiment. RASNIK alignment systems [8] can monitor the relative alignment of two 'alignment rods'. A set of these rods contains 2 RASNIK systems (see fig.8). A stick is fixed at each corner of a SuMo. A total of 576 systems of two-fold sticks will be needed.

As an alternative, tensioned thin wires could be used. This would allow the direct alignment of four chamber superlayers using one wire and four sensors, one for each superlayer. These systems may be more suitable for mass production. Another idea is to use silicon strip sensors in combination with infra-red lasers, as has been presented by ASCOT. Holes in the toroid iron are required for all of these options.

By means of a simulation the possibility of using muon data for obtaining the alignment should be studied. High momentum muons could be used which origin from single Z^0 decay. If the magnetic field in the iron can be made low enough, the distribution centroid of residual of track positions is a direct measure for the local alignment.

Detector Calibration

T-zero calibration

A simple test pulse on one wire for each group of about 16 wires within a chamber plane gives the T-zero differences per group. The differences within a group can be made small enough. Given the zig-zag drift directions, errors in the global T-zero do not cause a systematical error; a precision of 2 ns is sufficient.

Auto Calibration

The relation between the drift time and the drift distance can be obtained using muon data and/or cosmic ray data. Residual spectra selected in slices of the distance to the wire provide for the deviations of an assumed relation. Improved relations can be tried again and after some iterations the real relation is obtained. The global T-zero is another result of this procedure.

Strip preamp gain calibration.

The strip preamps are calibrated by measuring the response at the output of the ADCs of a charge injected in the strips. Only relative calibration matters; the calibration constants should be known to 0.5 percent in order to limit the local systematic error to 30 μm . The differences in charges, injected in the strips of one chamber layer should therefore be accurate to 0.2 percent. This is obtained by sacrificing one cell: in this cell a rigid, high precision 50 ohm coax cable is fixed at the cell centre line by means of foam. The core of this cable is grounded, while the calibration signal (a positive leading edge) is connected to the shield. The capacitive coupling between the coax cable and the strips depends only on the strip width which varies less than 0.2 percent (RMS). If the cable is off centre, the change in capacity is small since the capacity has a minimum at the cell centre. Moreover, only the ratio of calibration constants for three adjacent strips matters: a systematic change of capacity over the cable length has little influence.

The absolute calibration may be obtained using build-in ^{55}Fe sources.

Additional systems

HV systems. Only one positive HV potential for the wires is needed. There are no special demands for the stability. Since the chance of HV breakdowns is very little, the major part of the fan out may occur near the chambers. A modest number of cores is needed for the connections between the counting room and the experiment.

Gas system. The chambers may operate with a non-flammable gas. The demands on the stability of the mixing rate are modest.

Power supplies (low voltage). For the front end electronics, the ADCs and the TDCs, low-voltage power is needed. These supplies may be placed near the chambers, reducing the cable costs.

Cabling and tubing. It may be attractive to install and test all cables and tubes before the chamber modules.

Monitor systems. It may be needed to monitor the temperature, as well as the strength of the local magnetic field at several positions on the chambers. The analog data should be digitised on the chambers and the transputers should take care of the data transport.

Cooling. The strip preamplifiers and discriminators are expected to dissipate about 0.2 MW; a cooling system will be needed for this. Tubes for liquid cooling are integrated in the chamber design.

Data Acquisition. The digital data appears in registers behind the ADCs and TDCs. An additional register contains the hit addresses and the strip addresses carrying the largest signals. This data can be read out using shift registers and fifos.

A fast zero-dead time circuit is under development which read out all the registers without zero suppression. The data is compressed by the transputers. Additional transputers, grouped in sectors, should collect the data for the second level trigger. The trigger results will be communicated to the counting room transputers.

Off-line analyses. A database should contain the data of monolayer positions and RASNIK alignment data. The analyses of the track coordinate from the strip data is straightforward [1]; the coordinate obtained from the drift time measurements depends on the local geometry and magnetic field, temperature, pressure etc., and requires data samples for the 'auto-calibration' procedure.

Quantities

There are 18 different SuMo unit types, of which 9 are the mirror images of the other 9 (see fig.3). In total there are 18 times 16 = 288 SuMos.

MI 0

wire length: 2040 mm (supported in middle)
strip length: 4400 mm
area 8.97 m²
number of wires: 4160
number of strips: 2040

MI 1

wire length: 2040 mm (supported in middle)
strip length: 3000 mm
area 6.12 m²
number of wires: 2830
number of strips: 2040

MO 00

wire length: 3600 mm (supported in middle)
strip length: 3200 mm
area 11.52 m²
number of wires: 3020
number of strips: 3600

MO 01

wire length: 3600 mm (supported in middle)
strip length: 4200 mm
area 15.12 m²
number of wires: 3960
number of strips: 3600

MO 10

wire length: 3600 mm (supported in middle)
strip length: 2700 mm
area 9.72 m²
number of wires: 2550
number of strips: 3600

MO 11

wire length: 3600 mm (supported in middle)
strip length: 2700 mm
area 9.72 m²
number of wires: 2550
number of strips: 3600

FI

wire length: 300 - 2040 mm
strip length: 4200 mm
area 4.91 m²
number of wires: 3970
number of strips: 2040

FO 0

wire length: 500 - 2040 mm
strip length: 3600 mm
area 4.57 m²
number of wires: 3400
number of strips: 2040

FO 1

wire length:	2040 - 3600 mm
strip length:	3600 mm
area	10.15 m ²
number of wires:	3400
number of strips:	3600

Muon Station Surfaces

Barrel Inner Station	482	m ²
Barrel Outer Station	1474	m ²
Forward Inner Station	157	m ²
Forward Outer Station	471	m ²
total barrel	1956	m ²
total forward	628	m ²
TOTAL	2584	m ²

Numbers and length of wires, strips

Total wires	954 k
Total strips	873 k
Total wire length barrel	1856 km
total wire length forward	608 km
total wire length	2464 km

Material Cost Estimates

Most of the prices indicated here are quotes from industry. The prices will be more accurately known with time. In the 'pre-production phase', many of the design details must be discussed with potential producers in order to find the most cost effective solutions.

Chamber Materials

item	price/unit	total need	total costs
carbon facings	250 Sfr/m ²	10 k m ²	2500 kSfr
foil	20 Sfr/m ²	93 k m ²	1900 kSfr
hedgehog PCBs	50 Sfr/piece	30 k	1500 kSfr
Cu wire fix blocks	0.2 Sfr/piece	1908 k	380 kSfr
Cu/Be wire	0.15 Sfr/m	2464 km	369 kSfr
plastic end pieces	0.3 Sfr/piece	238 k	71 kSfr
Glass/PCB tube	5 Sfr/m	7 km	35 kSfr
other materials			500 kSfr
total chamber material costs			7255 kSfr

Readout Electronics

Wires

price per wire:

preamp+disc	4.
encoder	1

front PCB	1.
TDC	2
connectors etc	0.5
total per wire	8.5
total for 954 k wires	8109 kSf

Strips

price per strip	
preamp+ disc	6.
selector	1
front PCB	1.
ADC	3.
connectors etc	0.5
total per strip	11.5
total for 873 k strips	10039 kSf

DACQ Transputer system

Two transputers per SuMo + registers	500 kSf
Counting room electronics	500 kSf
transputers, racks, crates, supplies	
Total for readout electronics	19148 kSf

Others

Support mechanics	1000 kSf
Alignment systems	1000 kSf
Optical links for 288 SuMos and 64 level 2 trigger systems	300 kSf
HV systems incl. cabling and monitors	300 kSf
Gas system, incl. tubing	300 kSf
Power supplies (low voltage) incl. cabling	300 kSf
Cabling and tubing	300 kSf
Monitor and test systems	200 kSf
Cooling incl. tubing	200 kSf
Total for others	3900 kSf

total material and equipment costs for EAGLE, excl. RPCs: 30303 kSf

Labour Costs

Labour costs of one SuMo

Construction of typical monolayer of $3.5 * 3.5 \text{ m}^2$:	
folding of 4 foils	0.4 man-days
foil in template; alignment	0.4

end pieces fixing	0.6
wires on frames	0.8
wires in monolayer	0.8
foil in upper template	0.4
two templates together, ultrasonic welding	0.4
fixing planar foil	1.0
assembly strip end bar/PCB	0.4
fixing strip end bar/PCB	0.4
total	5.6
total for 12 monolayers:	67.2
monolayer assembly	8.
assembly RPC+inner+outer superlayers	10.
assembly & tests of electronics	10.
alignment, tests	10.
total	105.2
total for 288 SuMos:	30 000 (=137 man years)

These estimates can be verified during the production of four large HSC prototypes (P2) in 1992.

Production facilities

For the production of the SuMos one needs the following facilities:

	material (Sfr)	labour (man-y)
- a lower and an upper template	10 k	0.2
- vacuum equipment	5 k	0.1
- a foil folding machine	30 k	0.5
- a wire winding mill	10 k	0.5
- a flat assembly table	5 k	0.1
- ultra sonic weld equipment	20 k	0.2
- aux. tools, equipment	10 k	0.5
total	90 kSf	2.1

Other production items are the alignment systems and the support systems, as well as testing facilities for the chambers.

R & D

Gas. The demands of the gas mixture are:

- fast: low value of maximum drift time;
- reasonable Lorentz angle
- non-flammable

- non-toxic
- high cluster density

A compromise must be found.

EM shower effects.

The relation between the chamber geometry and the sensitivity for EM shower electrons should be studied. The results should be verified with muon detectors in RD5.

Triggers and Bunch Identifier.

Given the spatial resolution of the track coordinate obtained from the drift time measurement, the time resolution of a chamber layer is better than 5 ns after the track has been fitted. Consequently, the timing of the track should be known using the time information of all 16 or more layers passed by a muon. Algorithms for a level 1 Bunch Identifier should be studied and tested.

Preamps and Discriminators.

The large number of wires and strips require the development of ASICs.

Alternatives

Electronics.

If RPCs would provide for a level 1 trigger, the task of the HSC electronics would be just to read out the chamber signals. At present there are rapid developments in analog memories (Sample and Holds, analog shift registers, analog RAMs). As soon as massive accurate storage of instantaneous analog signals is possible, the electronics could consist just of preamp, sampling and storage sections. The relevant analog data could be collected after a trigger from the RPC detector.

FADC per strip. There are rapid developments in 'pipe-lined' 12-bit, low power FADC ASICs, to be applied for the readout of calorimeters. This FADC could sample a strip preamp pulse several times, thus limiting the effective preamp noise. The strip preamp can therefore be a simple and fast ASIC itself. Both the preamp and the FADC could be mounted at the end of each strip. The PCB in which they are mounted would only carry a digital bus and some power lines. The on-board transputer could act as digital filter and data compressor.

References

- [1] H.van der Graaf, A. König, G. Faber, T. Wijnen and P. Rewiersma: Nucl. Instr. & Methods A307 (1991) 220 - 230
- [2] K. Fujii et.al.: Nucl. Instr. & Methods 225 (1984) 23 - 30
- [3] F. Gasparini et. al.: Nucl. Instr. & Methods A267 (1988) 87 - 92
- [4] Y. Bonyushkin et. al.: EMPACT Note 358. Presented at IEEE Conference, Santa Fe, New Mexico, USA, Nov. 1991
- [5] S. Rescia et. al.: Monolithic JFET Charge Amplifier for Calorimetry at High Luminosity Hadron Colliders. Presented at IEEE Conference, Santa Fe, USA, Nov. 1991
- [6] R. Van Berg, University of Pennsylvania, USA. Presented at IEEE Conference, Santa Fe, New Mexico, USA, Nov. 1991
- [7] Report on RD5, 1992. CERN, January 1992, Geneva, Switzerland
- [8] Duinker, P.; Faber, G.; van der Graaf, H.; Groenstege, H.; Harting, D.; Hartjes, F.; Koopstra, J.; Leytens, X.; Massaro, G.; Onvlee, H.; Peng, Y.; Postema, H.; Rewiersma, P.; Vorenkamp, T.: Some methods and tools for testing and optimizing proportional wire chambers. Nucl. Instr. & Methods A273 (1988) 814-819

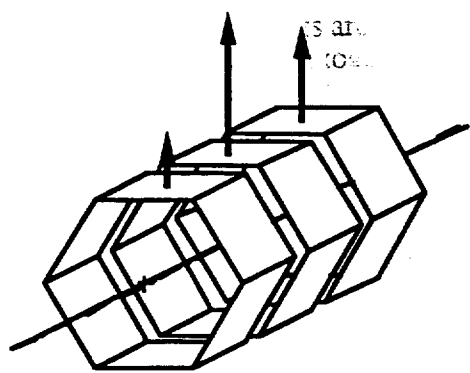


fig 1

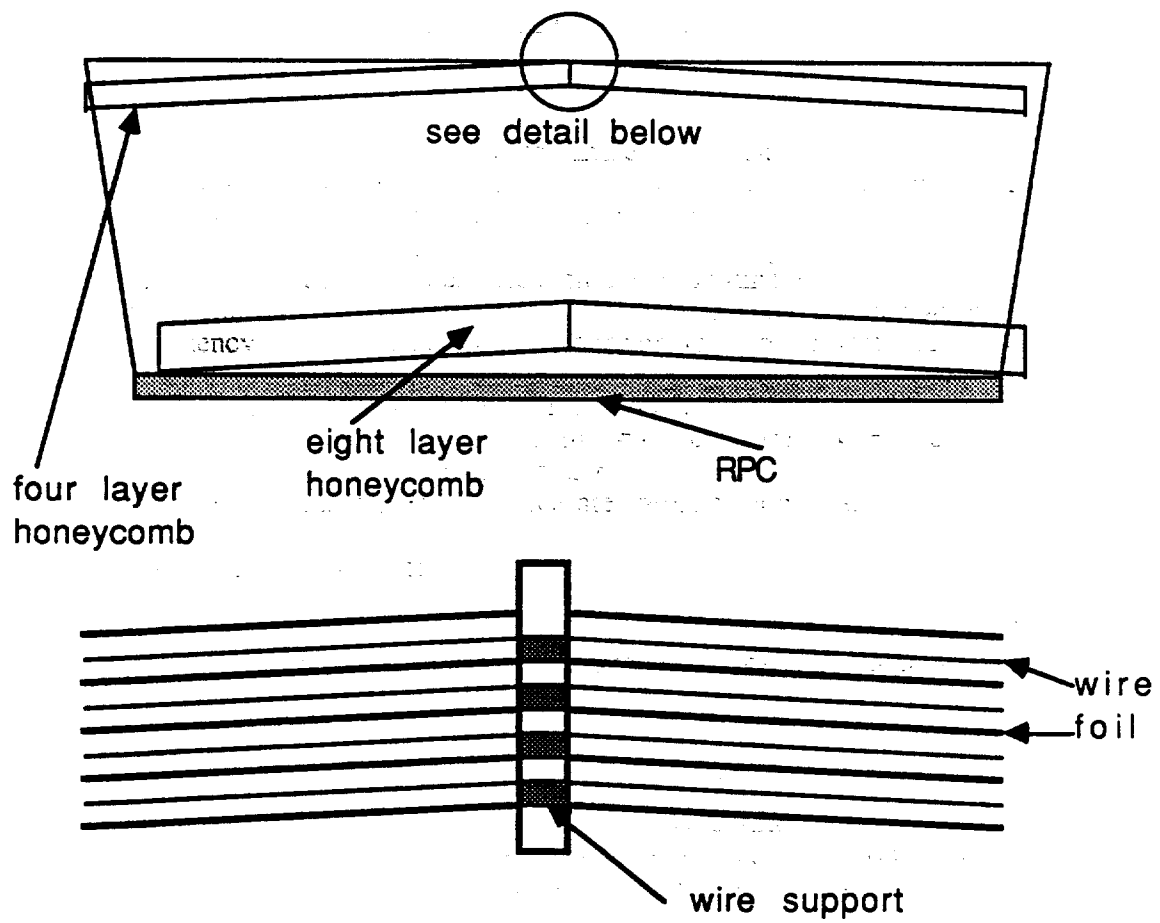


fig 2

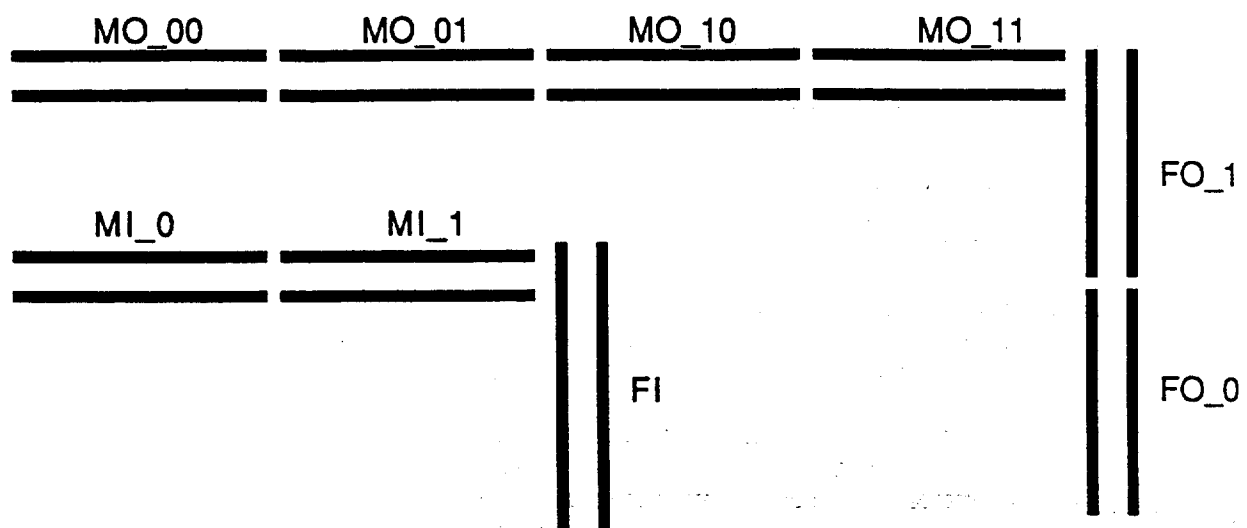


fig 3

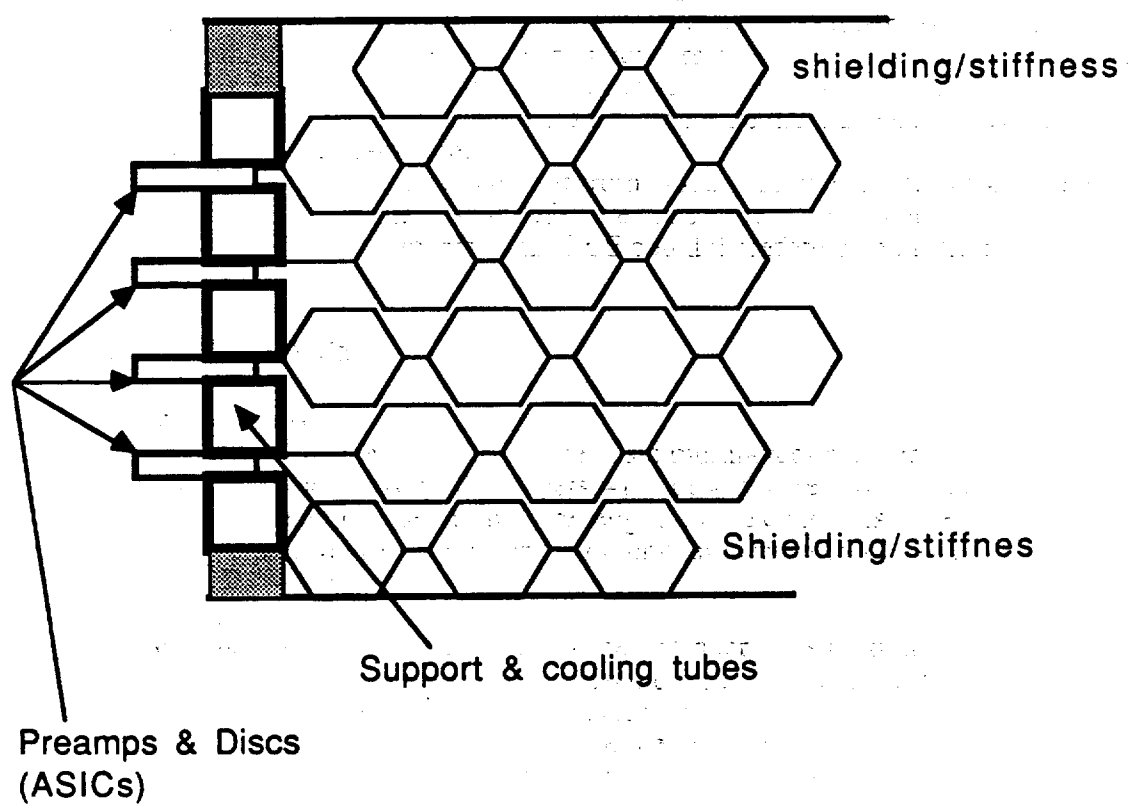


fig 4

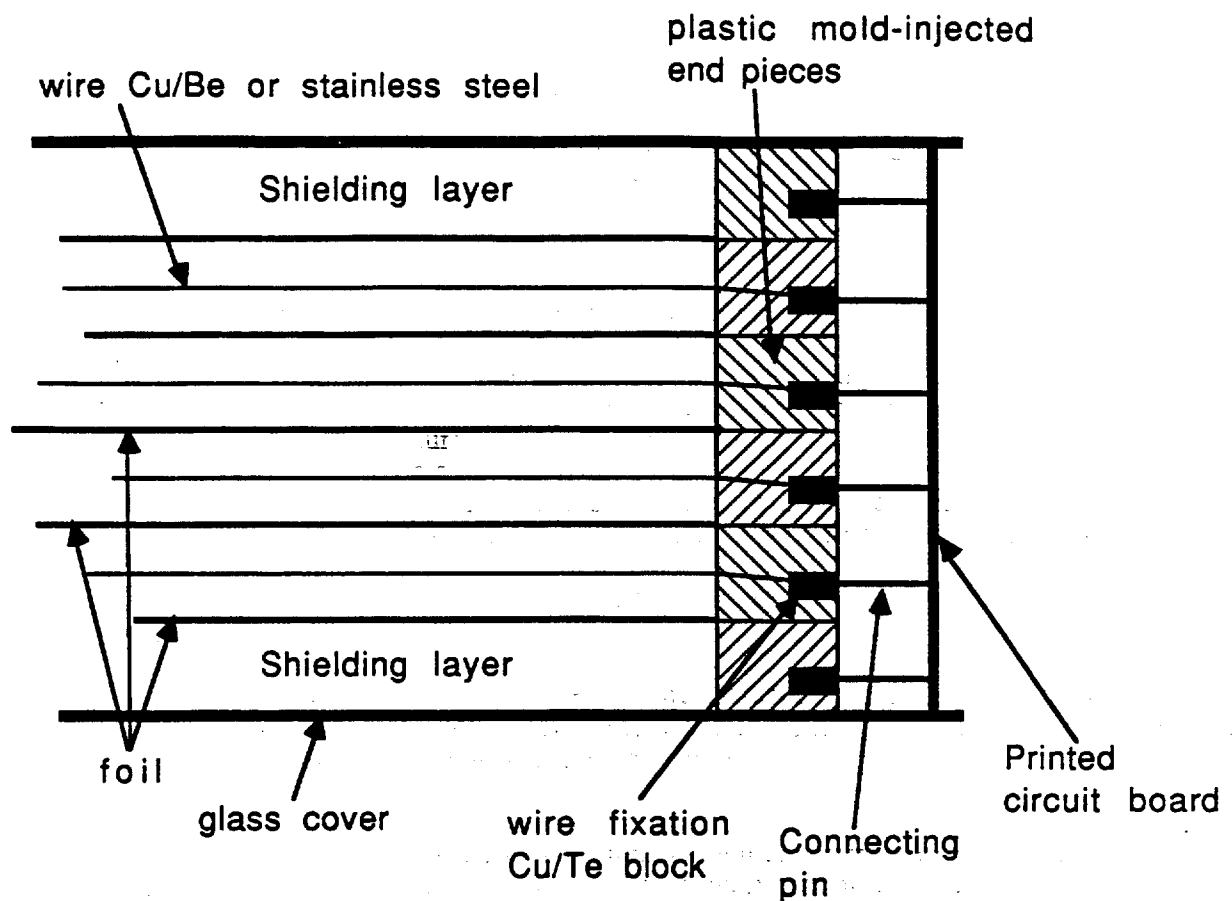


fig 5

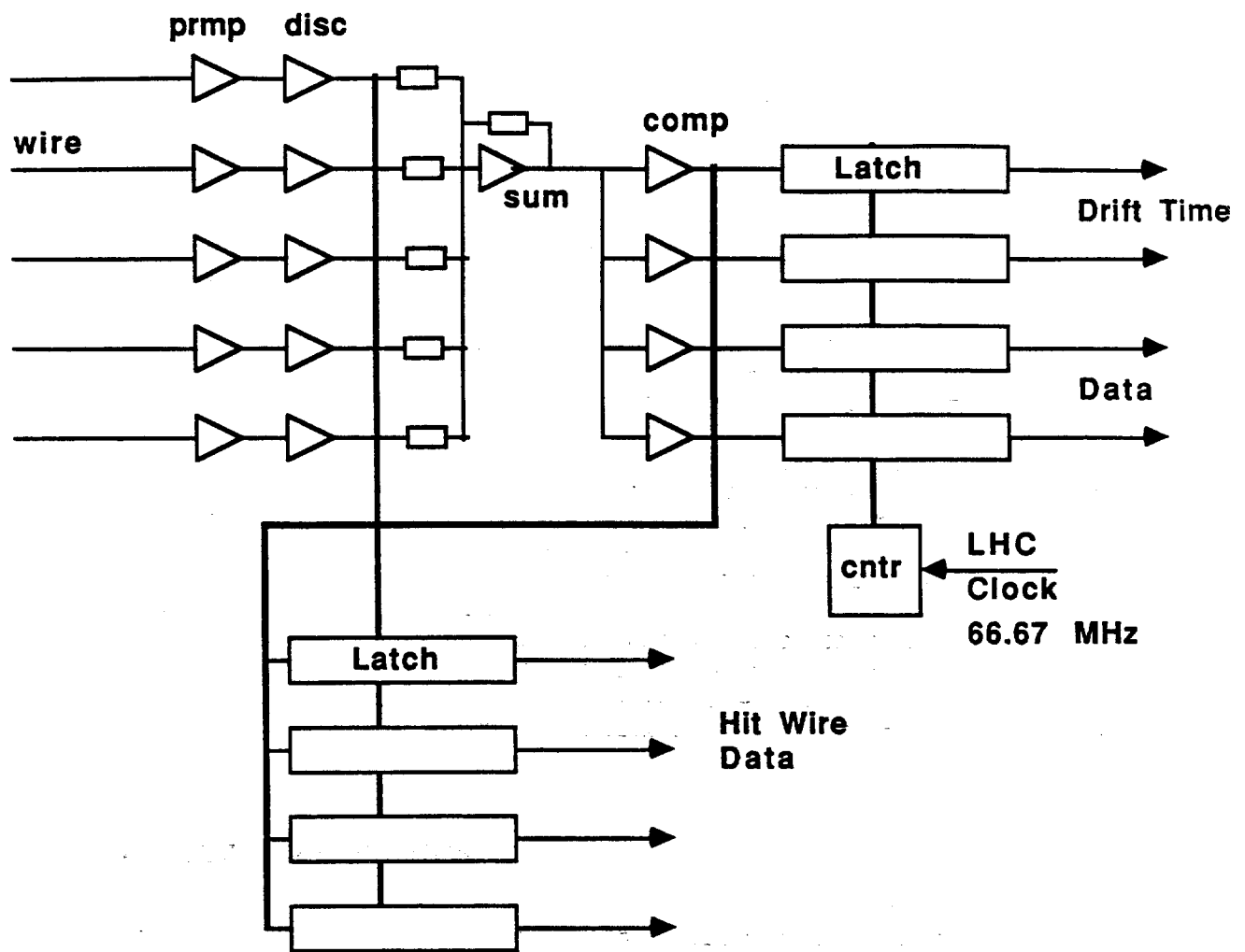


fig 6

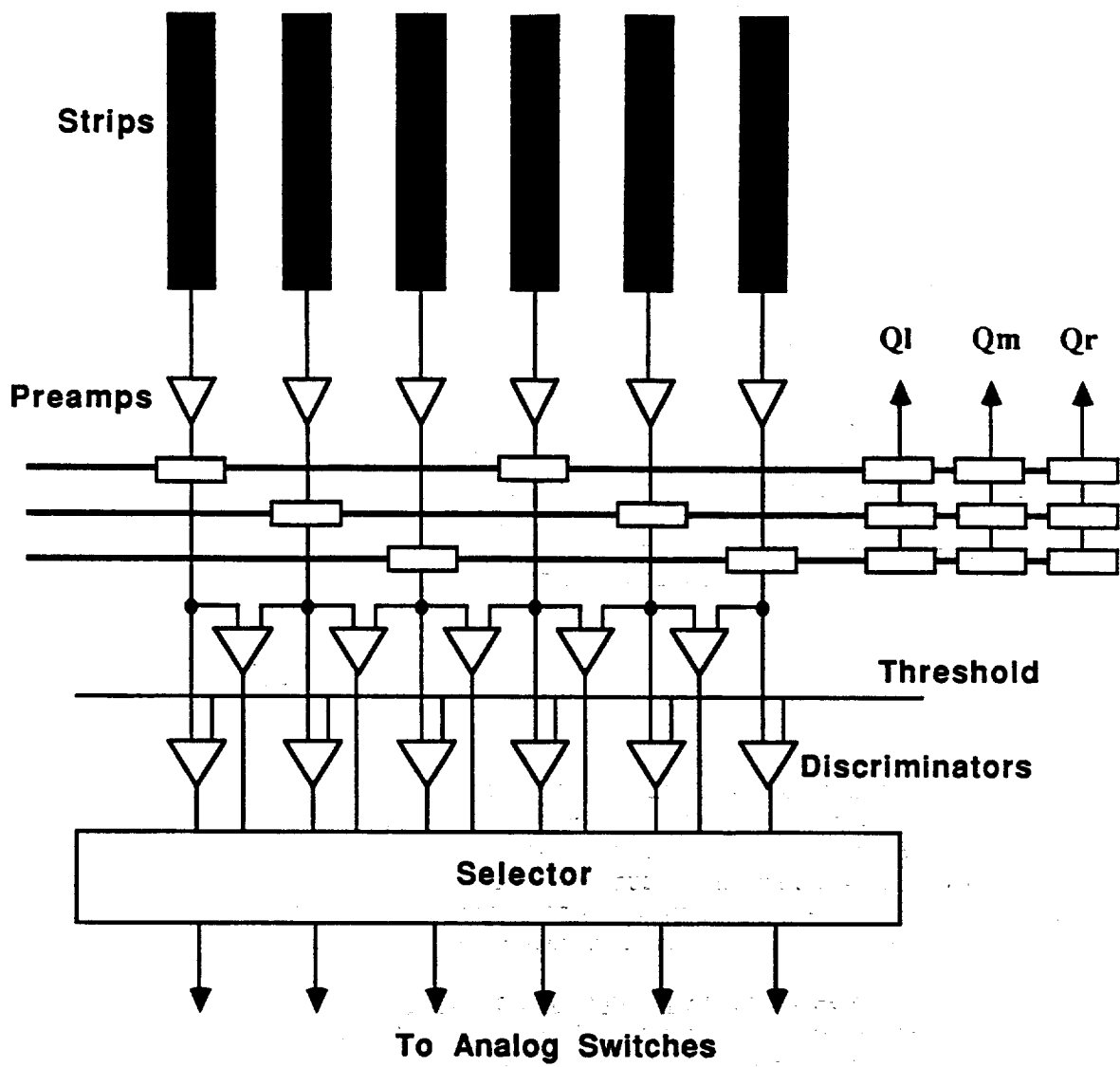


fig 7

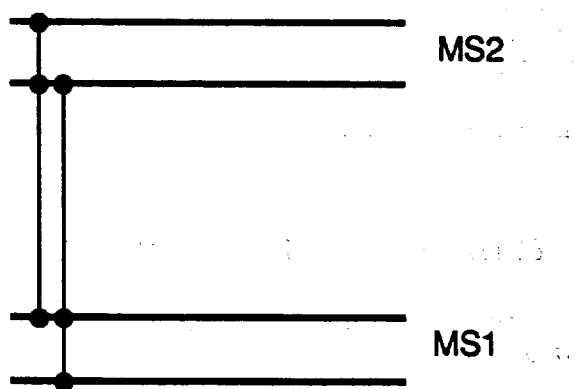
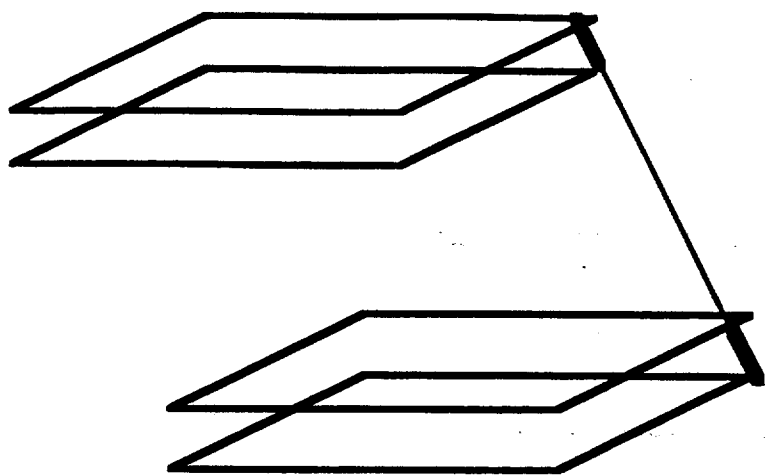


fig 8